Supporting information for

Critical Role of Defect State in the Photo-oxidation of Methanol on TiO_2(110)

Fan Jin[1,2†], Xiao Zhang[1†], Min Wei[1,3], Tingwei Chen[1], Huizhong Ma[1] and Yuchen Ma[1]*

[1]School of Chemistry and Chemical Engineering, Shandong University, Jinan 250100, China

[2]Department of Applied Chemistry, Yuncheng University, Yuncheng 044000, China

[3]School of Mathematics and Physics, Jinzhong University, Jinzhong 030619, China

[†]Authors contributed equally

*Corresponding author: myc@sdu.edu.cn

I. Convergence tests of GW and BSE calculations

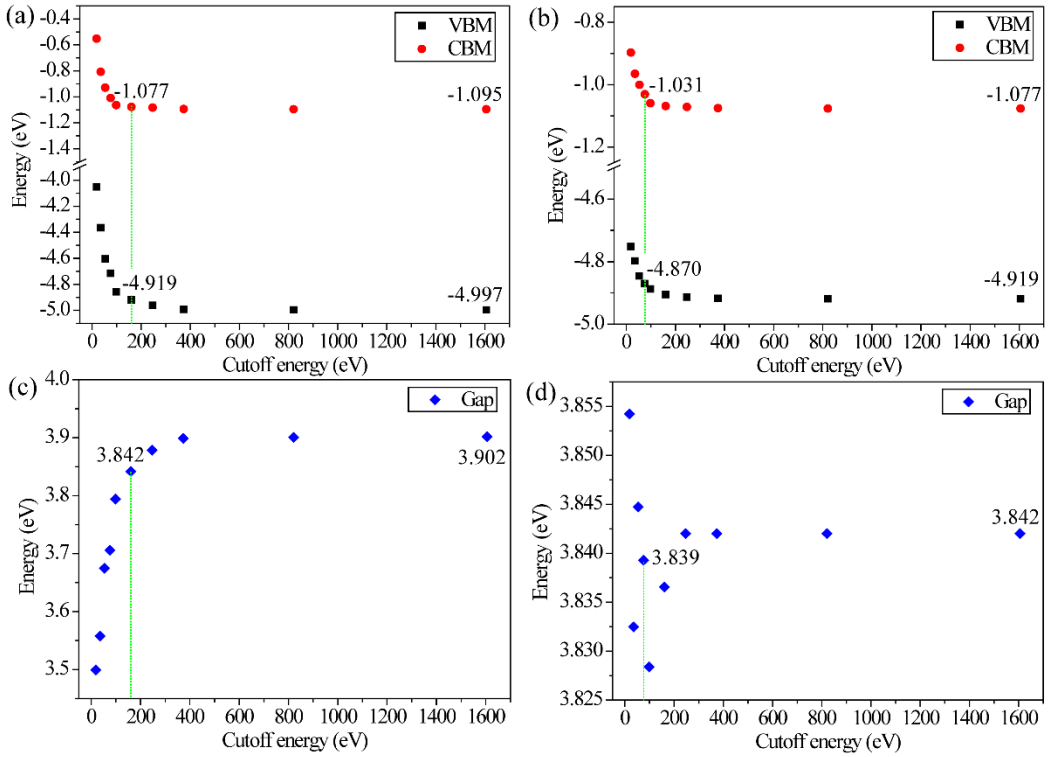

Figure S1. Evolution of VBM and CBM energies and the band gap at Γ point calculated by GW for the *CH_3OH/TiO_2 interface with the cutoff energy applied in the band summation over unoccupied orbitals for the evaluation of self-energy ((a) and (c)) and electronic screening ((b) and (d)). In the convergence test for self-energy, there is no cutoff in the evaluation of electronic screening. In the convergence test for electronic screening, cutoff energy is set to 160 eV in the evaluation of self-energy. The cutoff energies we adopt in realistic calculations are indicated by green vertical lines. Vacuum layer in the surface supercell is set to 30 Å.

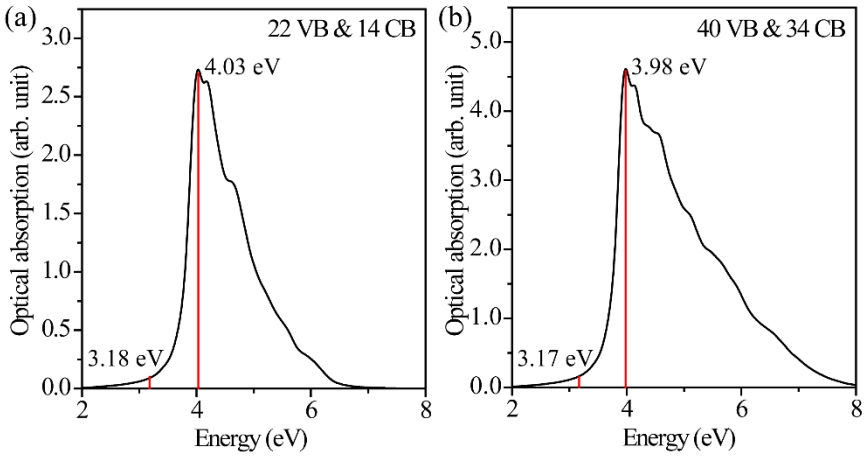

Figure S2. Optical absorption spectra of the *CH_3OH/TiO_2 interface calculated by BSE. (a) 22 valence and 14 conduction bands are included in BSE to represent exciton wave functions. (b) 40 valence and 34 conduction bands are included in BSE to represent exciton wave functions. A Gaussian broadening of 0.1 eV is employed in the spectra. A smaller *k*-point mesh of 8×8×1 is applied for the convergence test here due to the huge demand on CPU and memory for (b). To reduce the computational cost, different from the realistic calculations where the quasiparticle energy for each band at each BSE *k* point is evaluated by GW exactly, a rigid scissor shift, which is set to the energy difference between GW and LDA band gaps at Γ point, is applied to the occupied orbitals used in BSE for the convergence test here.

II. Electronic and excitonic properties of CH_3OH/TiO_2 interfaces

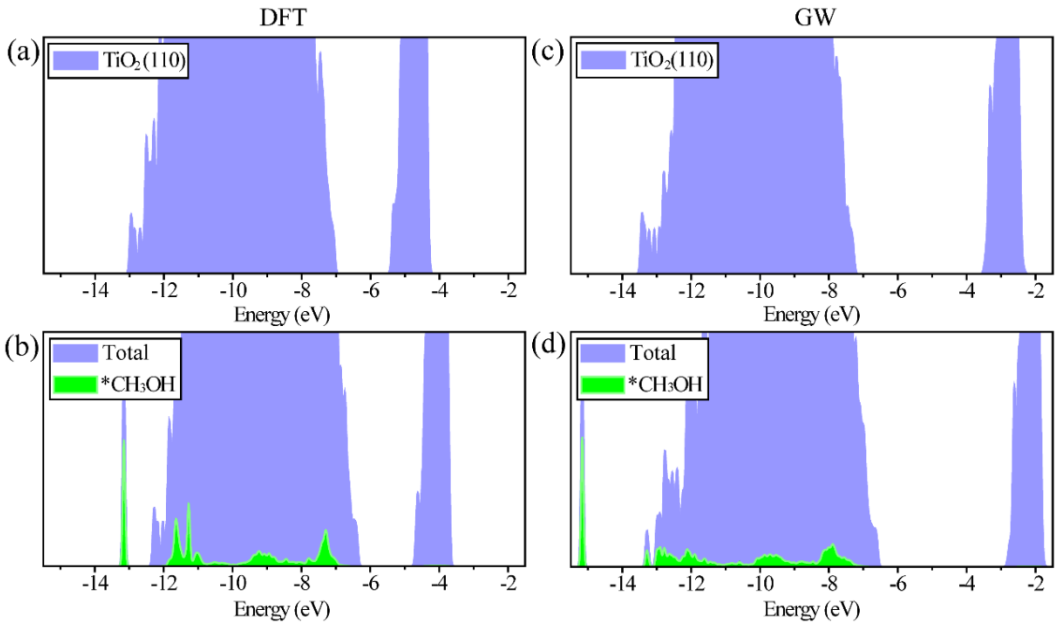

Figure S3. DOS of the clean TiO_2(110) surface calculated by DFT-LDA (a) and GW (c). Total and projected DOS of the $*CH_3OH/TiO_2$ interface calculated by DFT-LDA (b) and GW (d). Vacuum level is set to zero in each panel. In (c) and (d), the whole DOS has been shifted by 0.1 eV to lower energy owing to the error introduced by the band summation cutoffs in GW.

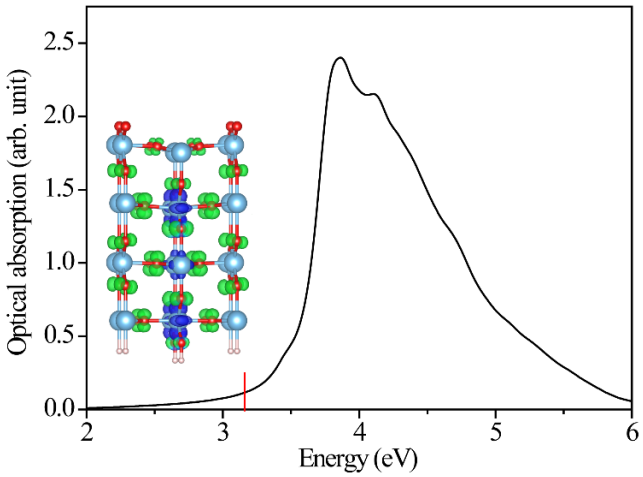

Figure S4. Optical absorption spectrum of the clean TiO_2(110) surface calculated by BSE. A Gaussian broadening of 0.1 eV is employed in the spectrum. The inset displays the spatial distribution of exciton (electron: blue isosurfaces; hole: green isosurfaces) for the lowest excited state which is marked by the vertical red line at 3.16 eV.

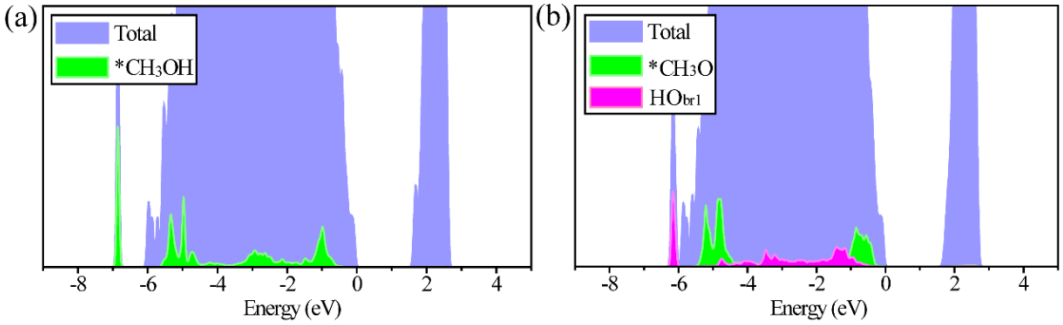

Figure S5. Total and projected DOS calculated by DFT-LDA for the *CH_3OH/TiO_2 (a) and the *CH_3O+HO_{br1}/TiO_2 (b) interfaces. VBM is set to zero in each panel.

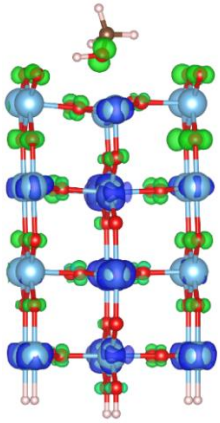

Figure S6. Spatial distribution of exciton (electron: blue isosurfaces; hole: green isosurfaces) for the excited state at 4.65 eV for the *CH_3OH/TiO_2 interface.

III. Structures and electronic properties of some intermediate states in the O-H and C-H dissociation processes

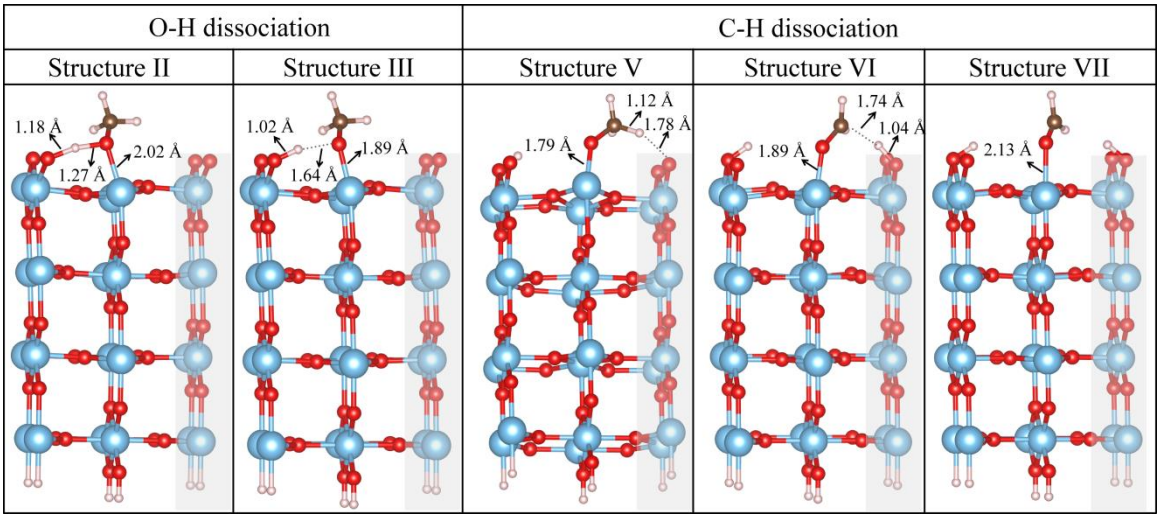

Figure S7. Structures of the intermediate states II, III, V, VI and VII (see Figure 3 of the main context) in the O-H and C-H dissociation processes. Light blue, red, brown and gray balls represent Ti, O, C and H atoms, respectively.

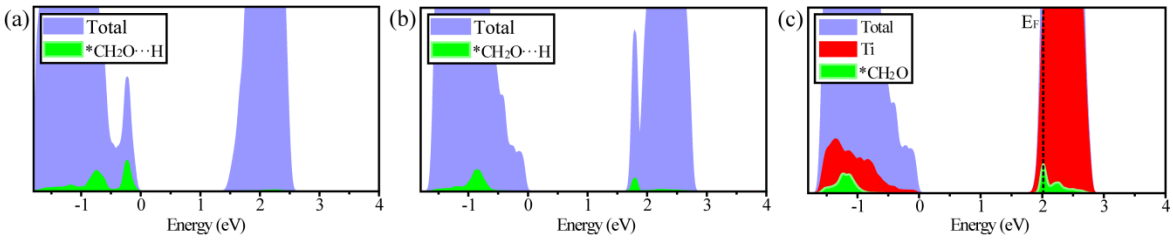

Figure S8. Total and project DOS calculated by DFT-LDA for the intermediate structures V (a), VI (b) and VII (c) (see Figure 3 of the main context) in the C-H dissociation process. VBM is set to zero in each panel. The Fermi level is marked by a black dashed line in (c).

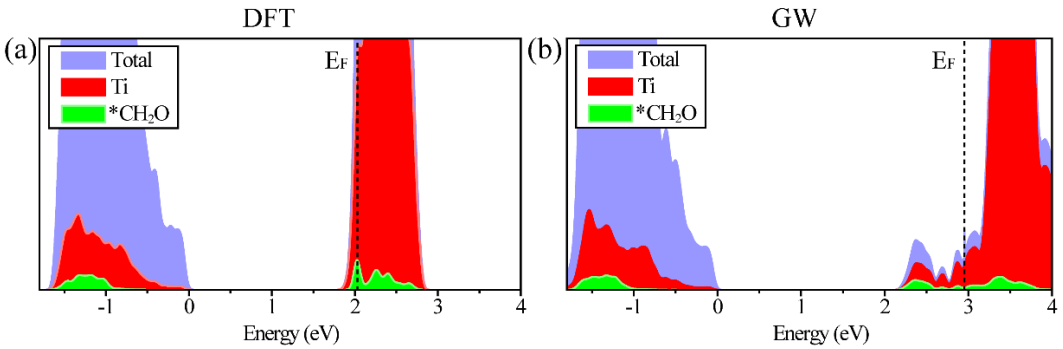

Figure S9. Total and projected DOS calculated by DFT-LDA (a) and GW (b) for structure VIII (see Figure 3 of the main context) in the C-H dissociation process. VBM is set to zero in each panel. The Fermi level is marked by black dashed lines.

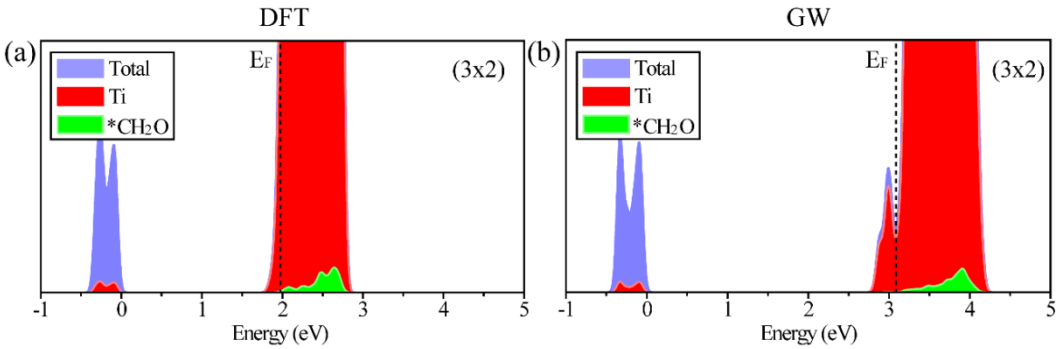

Figure S10. Total and projected DOS calculated by DFT-LDA (a) and GW (b) for the equivalent of structure VIII (see Figure 3 of the main context) in a (3×2) surface supercell. VBM is set to zero in each panel. The Fermi level is marked by black dashed lines.

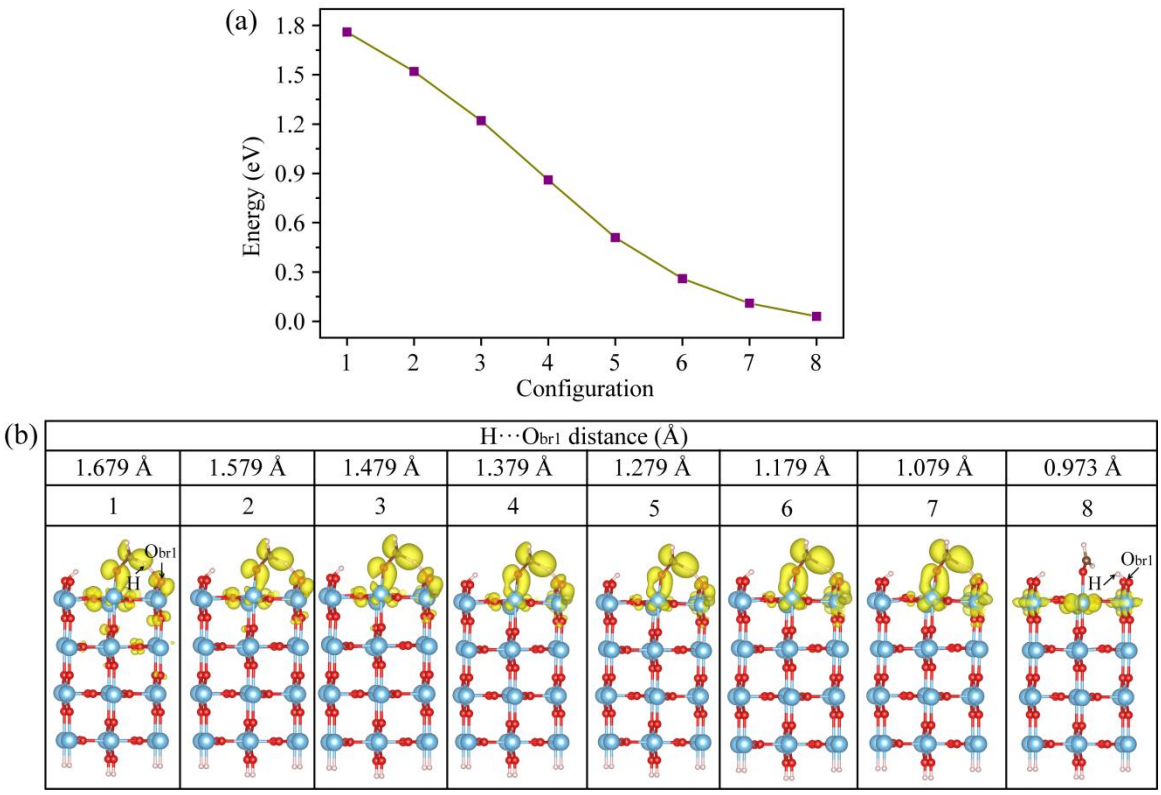

Figure S11. (a) Variation of the DFT-LDA gap between the filled defect level and CBM at Γ point along with the H transfer to O_{br1}. See panel (b) for the configurations. (b) Geometry and charge distribution of the filled defect level for the eight configurations. Configurations 1-8 are constructed by moving H of structure V in Figure 3 of the main context towards O_{br1} gradually, with their distance decreasing from 1.679 Å to 0.973 Å. In these configurations, positions of all atoms, except those of C, the transferred H, O_{br1} and the bottom O-Ti-O trilayer of the substrate, have been optimized by the VASP code.

IV. Convergence test on the thickness of the surface slab model

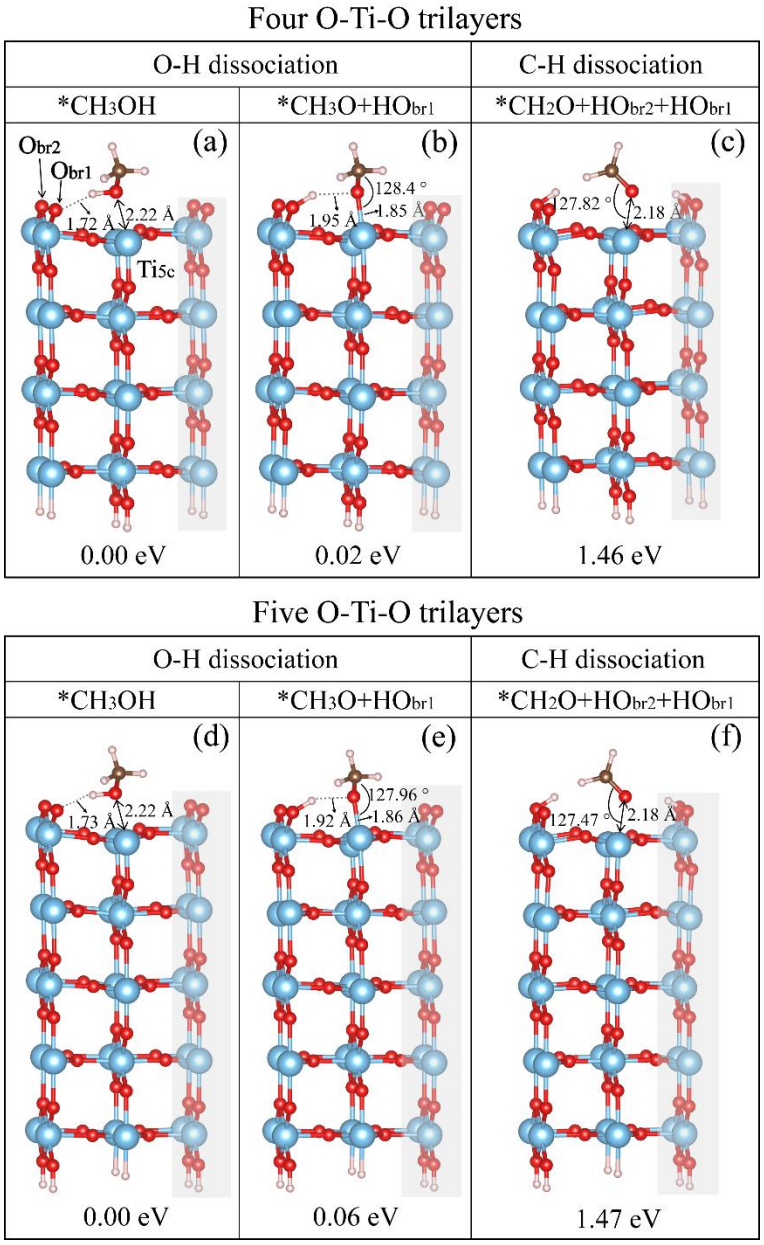

Figure S12. Relative energies of the products in the O-H and C-H dissociation reactions with respect to the initial reactant. (a-c) Slab model constructed by four O-Ti-O trilayers. (d-e) Slab model constructed by five O-Ti-O trilayers. Some bond lengths and bond angles are presented for comparison.

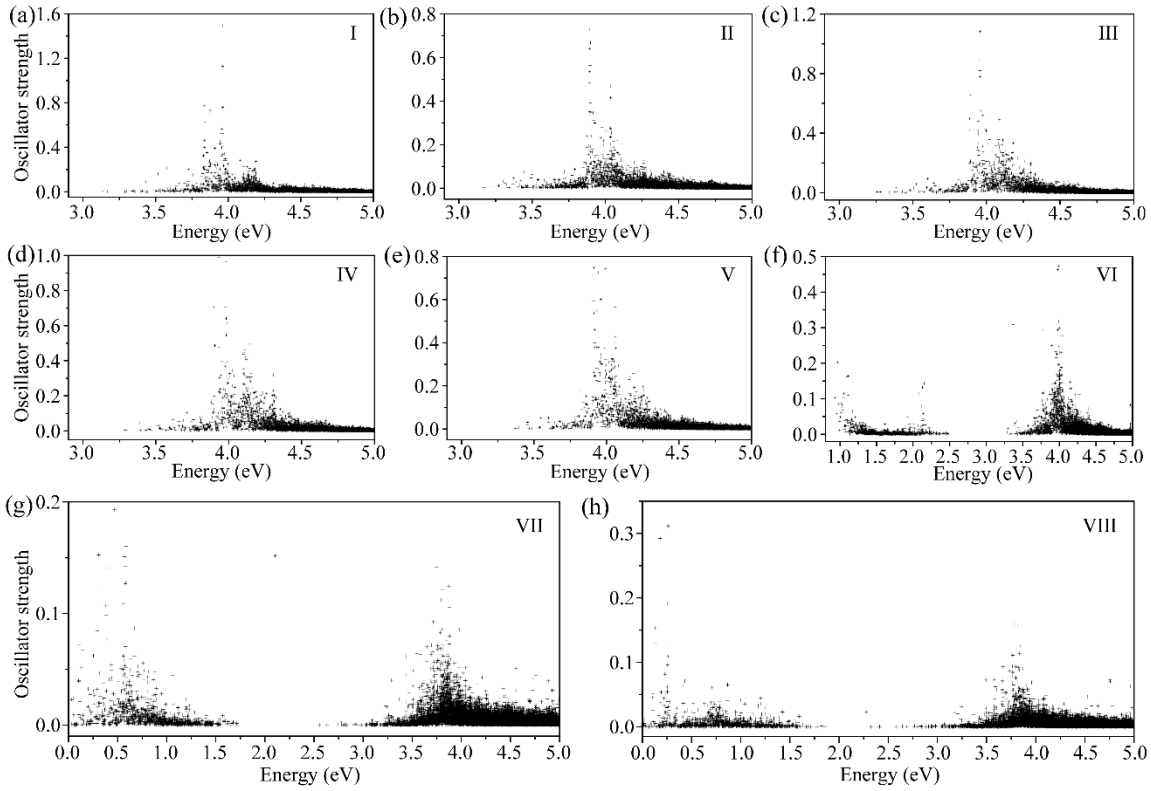

Figure S13. Energies and oscillator strengths (denoted by crosses) computed by BSE for all the optical excitations below 5.0 eV for the structures I to VIII shown in Fig. 3 of the main context. Direction of the incident light is set to be along the normal of TiO_2(110) surface.